Journal of Zhejiang University-SCIENCE A (Applied Physics & Engineering)
ISSN 1673-565X (Print); ISSN 1862-1775 (Online)
www.zju.edu.cn/jzus; www.springerlink.com
E-mail: jzus@zju.edu.cn

Two-parameter characterization of low cycle, hysteretic fatigue data*

Sheng BAO†1, Wei-liang JIN[1], Sidney A. GURALNICK[2], Thomas ERBER[3,4]

([1]*Institute of Structural Engineering, Zhejiang University, Hangzhou 310058, China*)

([2]*Department of Civil Engineering, Illinois Institute of Technology, Chicago, IL 60616, USA*)

([3]*Department of Physics, Illinois Institute of Technology, Chicago, IL 60616, USA*)

([4]*Department of Applied Mathematics, Illinois Institute of Technology, Chicago, IL 60616, USA*)

†E-mail: longtubao@zju.edu.cn

Received Dec. 14, 2009; Revision accepted Mar. 23, 2010; Crosschecked Apr. 28, 2010

Abstract: The aim of this research is to characterize the development of fatigue damage by means of stress-strain hysteresis. Experiments were conducted on 14 specimens made of cold-finished unannealed AISI 1018 steel. Results demonstrate that the mechanical hysteresis loop areas, when plotted as a function of the number of loading cycles, show significant variations and demonstrate the three principal stages concerning the progress of the fatigue failure—initial accommodation, accretion of damage and terminal failure. These three stages of fatigue are marked by the transitions at cycles N_2 and N_3. Experimental results show that although fatigue life N_f ranges from 2644 cycles to 108 992 cycles, the ratios of N_2/N_f and N_3/N_f tend to be stable: N_2/N_f=10.7%, N_3/N_f=91.3%.

Key words: Hysteresis loss, Fatigue life, Fatigue damage
doi:10.1631/jzus.A0900763 **Document code:** A **CLC number:** TB302.5

1 Introduction

Metal fatigue is a result of cumulative damage due to repeated cyclic loadings which cause premature failure. The fatigue failure in metals subjected to cyclic loading is a random, progressive and cumulative damage process occurring at the microscopic and mesoscopic level (Kachanov, 1986; Bannantine *et al.*, 1990; Lemaitre and Chaboche, 1990; Bily, 1993). Many of the characteristics of fatigue damage, such as dislocation motion, occur in the range of dozens to hundreds of atoms in size. Due to the random nature and small size of the damage, observation of the critical sites is extremely difficult, if not impossible, with either scanning electron microscope (SEM) or conventional transmission electron microscope (TEM) techniques (Dieter, 1988). As a result, indirect techniques rather than direct measurements are used to study the damage that occurs in the fatigue process. A common indirect indicator of the progress of the fatigue process is the evolution of energy from mechanical hysteresis (Erber *et al.*, 1993).

The most notable attempt at predicting how damage accumulates during cyclic loading was proposed by Miner (1945). Miner's law of cumulative damage is usually expressed as

$$\sum_{i=1}^{k}\frac{n_i}{N_i}=1, \tag{1}$$

where n_i is the number of cycles at the ith stress amplitude, N_i is the number of cycles to cause failure at the ith stress amplitude, and k is the total number of different stress amplitudes. Failure occurs when the sum of the k cycle ratios is equal to 1. Eq. (1) was originally derived by Miner (1945) with an energy approach, in which a linear variation of the ratio of

* Project supported by the National Natural Science Foundation of China (No. 50901067), the Technological Research and Development Programs of the Ministry of Railways of China (No. 20101007-EG), and the Julian S. SCHWINGER Foundation, USA

energy per cycle to total energy to failure was assumed. Feltner and Morrow (1961) and Martin (1961) proposed that the total energy required to fracture a specimen under monotonic tension is equal to the amount of damaging energy required to cause failure in fatigue. Halford (1966) compared the thermal energy required to melt iron with the total energy accumulated over a fatigue life of 500 000 cycles. He concluded that the equivalent thermal energy lost over 500 000 cycles is more than nine times the energy required to melt the steel. The total mechanical hysteresis exhibited by a metal subjected to cyclic loading can be split into two parts. One part, which is large, is converted into thermal energy and is harmlessly dissipated into the environment during the loading history of the material. The other part, which is less than 1% of the total hysteresis energy, leads to the accumulation of fatigue damage in the material, which, if indefinitely prolonged, will result in complete rupture (Erber *et al.*, 1993; Erber, 2001). This disparity shows why it is so difficult to obtain direct information concerning fatigue damage from an individual hysteresis loop. Nevertheless, the fatigue failure process is paralleled by systematic changes of the hysteresis loops which may be manifest over intervals of hundreds or thousands of cycles. Experimental results demonstrated that measurements of hysteresis can yield significant insights into various stages of the development of a fatigue critical microstructure which culminated in complete rupture of the material.

2 Experiments

An MTS-810 servohydraulic fatigue testing machine controlled by an MTS 458.20 MicroConsole is used to apply cyclic tension and compression. Load values are derived from a force transducer with 0.03% full scale accuracy. A standard 1.27 cm gauge length MTS extensometer is used to measure strain. Over a maximum strain range of ±0.15, the hysteresis and nonlinearity of this gauge are 0.10% and 0.15%, respectively. A desktop computer equipped with a National Instruments coprocessor board and LabView software was used for data acquisition. Analog signals were first captured by sensors and then collected in the National Instruments SCB-68 68-Pin Shielded Connector. Afterwards, they were converted into digital input signals by a PCI-MIO-16XE-10 data acquisition card. Schematization of the data acquisition flow chart is shown in Fig. 1. A more detailed description of the experimental procedures can be found in (Erber *et al.*, 1993; 1997; Guralnick *et al.*, 2008) and (Michels, 1991; Desai, 1994; Agar, 1998; Berktan, 1998; Bao, 2004; 2007).

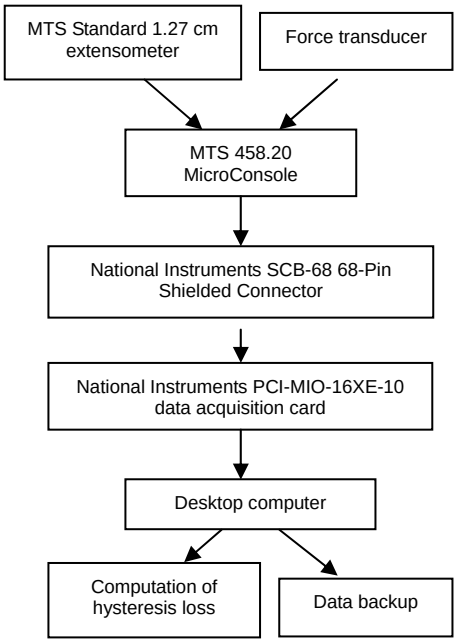

Fig. 1 Data acquisition flow chart

All of the experiments were run under strain control with symmetric triangular profiles to simplify the calculation of the hysteresis loop areas. A ramping rate of 2 s per cycle and a sampling rate of 50 data points per cycle were used for all of the tests. However, data points sampled at a rate of 49 points per cycle also occurred in the tests (Bao, 2004). This is because the speed of the MicroConsole output analog signals could not be exactly synchronized with the computer's processing speed. To post-process the data, customized computer programs were used to calculate the hysteresis loop areas and to plot all of the analyzed data.

All of the fatigue specimens were machined from a single bar of cold-finished unannealed AISI 1018 steel and the specimen dimensions are shown in Fig. 2. This material was selected because extensive data on its performance exists in the engineering literature and its stress-strain curve is of the gradual yielding type. It mirrors at least the monotonic stress-strain behavior of

many kinds of metals that used in the aircraft industry. Table 1 shows the nominal chemical composition of this material. Ten ASTM type 2 axial tension specimens were fabricated and loaded to failure. The mechanical properties obtained in these ten tests are listed in Table 2. These results are consistent with those described in the American Society for Metals (II-1986) (1986). In Table 2, the endurance limit is estimated from the ultimate stress, i.e., endurance limit is less than half of the ultimate stress.

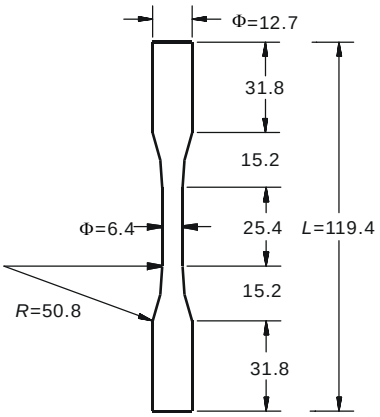

Fig. 2 Fatigue specimen dimensions (unit: mm)

Table 1 Chemical composition of AISI 1018 steel

Element	Percentile weight	Element	Percentile weight
Carbon	0.16	Nickel	0.04
Manganese	0.75	Chromium	0.04
Phosphorous	0.012	Copper	0.06
Sulfur	0.016	Molybdenum	0.02
Silicon	0.04	Iron	98.86

Table 2 Mechanical properties of AISI 1018 steel

Parameter	Value
Modulus of elasticity	202–207 GPa
Proportional limit	330–360 MPa
0.2% offset yield strength	450–480 MPa
Ultimate tensile strength	520–550 MPa
Endurance (fatigue) limit	<262 MPa

3 Computation of hysteresis loop area

The obtained stress and strain data was used to compute the hysteresis loop areas which correspond to the irrecoverable energy loss. The computation of the hysteresis loop area is based on the trapezoidal rule which is given as

$$U_p = \sum_{i=1}^{n_d} \Delta U_i(\varepsilon) \cong \sum_{i=1}^{n_d} \frac{1}{2}(\sigma_i + \sigma_{i-1})(\varepsilon_i - \varepsilon_{i-1}), \quad (2)$$

where U_p is the hysteresis loop area of the pth test cycle, $\Delta U_i(\varepsilon)$ is the hysteresis loop area increment for the ith data point in a particular test cycle, n_d is the number of data points in a particular test cycle, σ_i and σ_{i-1} are the stress values corresponding to respective data points, and ε_i and ε_{i-1} are the strain values corresponding to respective data points. This method of calculating the hysteresis loop areas using the trapezoidal rule can also be found in (Giancane *et al.*, 2010). Fig. 3 illustrates the computation of the hysteresis loop area by the summation of the four shaded areas A_1, A_2, A_3 and A_4. One can obtain from Fig. 3 that A_1 and A_3 are negative values, while A_2 and A_4 are positive values. Thus, the hysteresis loop area can also be written as

$$U_p = A_2 + A_4 - |A_1| - |A_3|. \quad (3)$$

It is difficult to define a hysteresis loop because of a lack of a consistent sampling rate. A sampling rate of 50 data points per cycle was used for all of the tests herein. However, the speed of the MicroConsole output analog signals could not be exactly synchronized with the computer's processing speed. As a result, a sampling rate of 49 data points per cycle also occurred during approximately every 3 or 4 test cycles in all of the experiments. With the experiments increased to thousands of cycles, this introduced a difficulty in selecting hysteresis loop points for every cycle. To solve this problem, strain was used as a control value to define a loop. In Fig. 4, the strain first increases to a maximum local value and then decreases to a minimum local value thus creating a triangular waveform. The point where $\Delta\varepsilon_i$ changes from a negative value to a positive value may be used as a control point to divide these two cycles. In this figure, point e is used as the control point that divides cycle 415 and cycle 416 of test Fts013.

Owing to the discretization of the data, some caution is necessary in computing the hysteresis loop

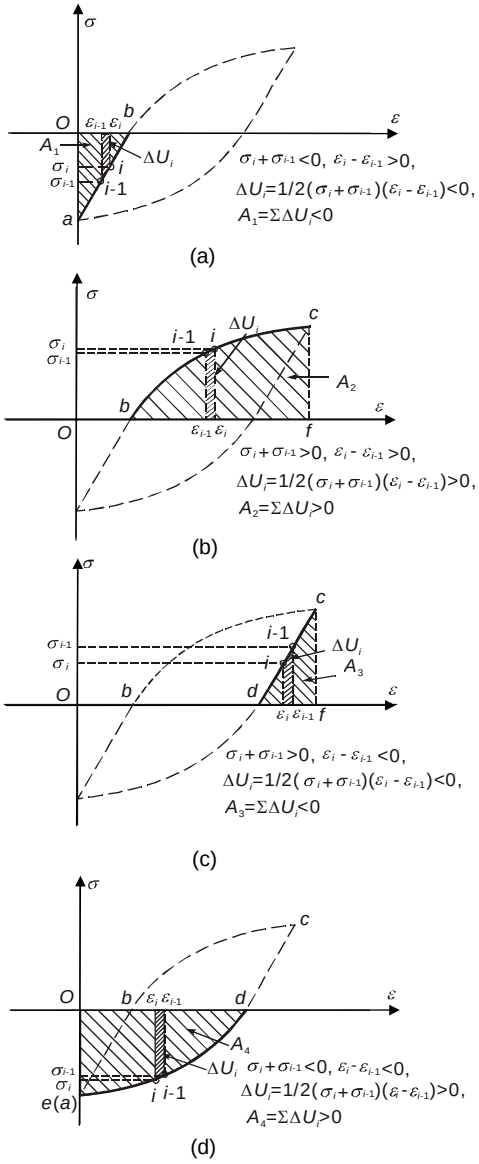

Fig. 3 Computation of hysteresis loop areas. (a) A_1; (b) A_2; (c) A_3; (d) A_4

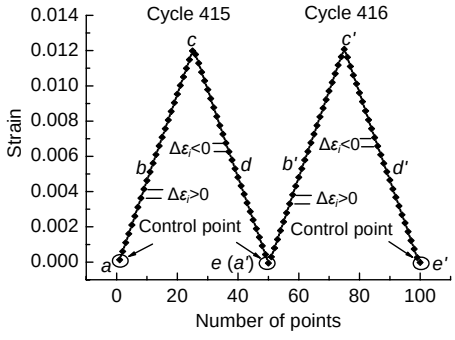

Fig. 4 Strain diagram of cycle 415 and cycle 416 of test Fts013

area. In Fig. 5, the area calculated using Eq. (3) is actually the summation of the hysteresis loop area and area ΔA_1 instead of just the loop area. An error of ΔA_1 was introduced because the experimental data of stress and strain do not produce closed hysteresis loops. The nonclosure of the hysteresis loops is due to the fact that the load application of the MTS system cannot be synchronized with data sampling. The calculated value of ΔA_1 can be positive or negative thus causing the hysteresis loss vs. the number of cycles curve to fluctuate as shown in Fig. 6a. One way to reduce this error is to move the hysteresis loop up along the stress axis so that the area of ΔA_1 is

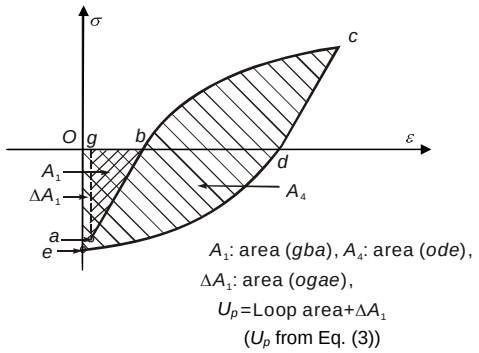

Fig. 5 Hysteresis loop area and ΔA_1

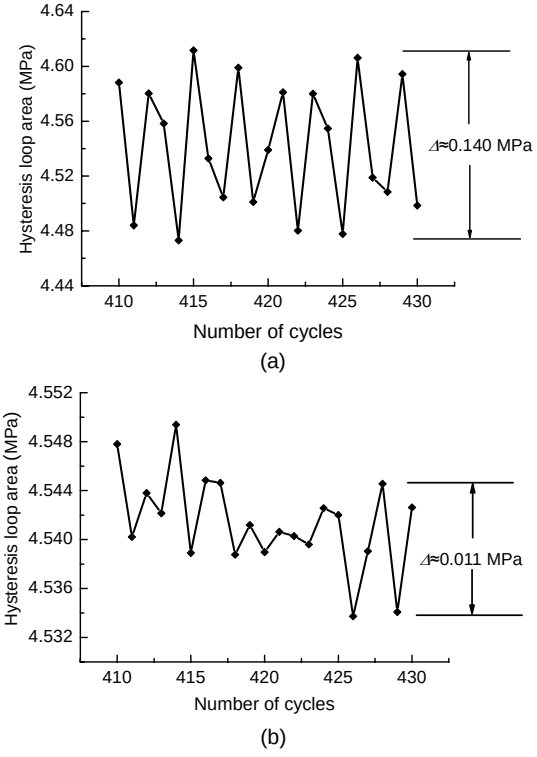

Fig. 6 Hysteresis loss fluctuation of test Fts013 with hysteresis loops (a) unshifted and (b) shifted up

nullified. From Fig. 6a, one may observe that the hysteresis loss vs. the number of cycles curve has a maximum fluctuation (Δ) of about 0.140 MPa before the hysteresis loops were moved up. This value is reduced to about 0.011 MPa after the hysteresis loops were moved up as shown in Fig. 6b.

4 Results and conclusions

Fig. 7 shows a typical graph of the hysteresis loop areas plotted against the number of loading cycles. It can be clearly found that the fatigue degradation process consists of three stages. The first part of the hysteresis loss curve decreases quickly corresponding to the material's drastic intrinsic adjustment to the external loading. This is referred to as initial accommodation. Then the hysteresis curve reduces in magnitude to a stage with a more gradual rate of change known as the accretion of damage regime. With the number of loading cycles increasing, the damage accumulates resulting in the alteration of the mesostructure of the material. The final stage of fatigue is indicated as the sharp down turn of the hysteresis loop area curve. In this stage, the microcracks propagate and join together, finally leading to the complete rupture of the specimen. The hysteresis loss curve is marked by the transitions at N_2 and N_3 cycles as shown in Fig. 7. To determine the transition points N_2 and N_3, a simple curve was fitted to each of the three principal stages and the two intersection points of these three curves are marked as N_2 and N_3. The most detailed description of this method for locating N_2 and N_3 values is given in (Guralnick *et al.*, 2008). The analyzed N_2 and N_3 values for all of the tests are listed in Table 3. Extensive studies show that although the specific N_2 and N_3 values may change drastically from test to test, the ratios of N_2/N_f and N_3/N_f tend to be stable. In Table 3, we can find that the fatigue life N_f of the 14 tests spans the range from 2644 cycles to 108 992 cycles and that N_2 and N_3 values vary accordingly. Nevertheless, N_2 and N_3 have an approximately invariant relation to the final fatigue failure at N_f: N_2/N_f=10.7% and N_3/N_f=91.3%. This apparent invariance implies that N_2, together with the loading program, can essentially determine the fatigue life N_f.

It is well known that the fatigue process is very sensitive to the slight variations in the initial states of the specimens, and that these differences are amplified by the repetitive application of external loads. Because of this complex behavior, the only way to improve the prediction of fatigue life is to find some indices of performance during the early loading period of a particular specimen that forecast its fatigue life N_f. It is useful to consider N_2 as an early warning of a specimen's fatigue life N_f, i.e., $N_f \approx 9.3N_2$. When the fatigue process approaches the transitional point N_3 of the later fatigue stage, further observations can improve the fatigue life prediction, i.e., $N_f \approx 1.1N_3$.

Another important result of this experiment is that the hysteresis loss per cycle is essentially a constant as shown in Fig. 7. This is true with the exception of the initial and the final spans of cycles which do not exceed 10% of N_f. Fig. 8 shows a typical graph of the cumulative hysteresis loop areas vs. the

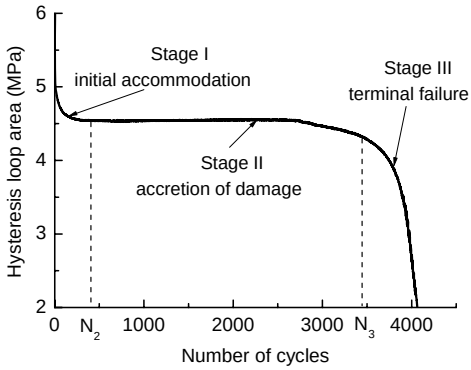

Fig. 7 Stress-strain hysteresis loop areas vs. the number of cycles for test Fts013

Table 3 Fatigue test results

Test	Strain range	N_f	N_2	N_2/N_f (%)	N_3	N_3/N_f (%)
Fts012	0.0135	2644	307	11.6	2408	91.1
Fts013	0.0120	4101	361	8.8	3772	92.0
Fts023	0.0110	4282	460	10.7	3887	90.8
Fts014	0.0105	5695	601	10.6	5383	94.5
Fts020	0.0100	6165	749	12.1	5425	88.0
Fts015	0.0090	9348	867	9.3	8655	92.6
Fts021	0.0082	8841	804	9.1	7628	86.3
Fts016	0.0075	14582	1237	8.5	12880	88.3
Fts022	0.0068	16013	1732	10.8	14843	92.7
Fts017	0.0060	30687	3312	10.8	27630	90.0
Fts025	0.0053	44570	5023	11.3	39604	88.9
Fts026	0.0050	56149	7177	12.8	51960	92.5
Fts027	0.0044	79619	9146	11.5	74502	93.6
Fts029	0.0040	108992	12225	11.2	105226	96.5
Average				10.7		91.3

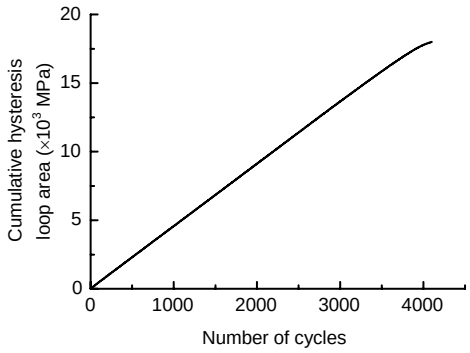

Fig. 8 Cumulative hysteresis loop areas vs. the number of cycles for test Fts013

number of cycles, which is essentially a straight line. This indicates that the hysteresis loss per cycle has nearly a constant value and the accumulated total hysteresis energy is a linear function of the number of cycles of load application for nearly the entire loading history to the final rupture. If the total hysteresis energy may be split into two parts, one part being harmlessly dissipated as heat and the other part causing the accumulation of damage, then the latter part is a constant for each cycle and the total damaging energy also accumulates as a linear function of the number of cycles of load application (Peyroux *et al.*, 1998; Chrysochoos *et al.*, 2008; Giancane *et al.*, 2009). This result indicates that combining acoustic emission measurements, hysteresis measurements and post-mortem examinations of ruptured specimens may lead to new insights concerning the origin and inception of the fatigue process in metals.

References

Agar, B.B., 1998. Hysteresis and Low Cycle Fatigue in Selected Aluminum Alloys. MS Thesis, Illinois Institute of Technology, Chicago, IL.

American Society for Metals (II-1986), 1986. Metals Handbook. Carnes Publication Services Inc., USA.

Bannantine, J.A., Comer, J.J., Handrock, J.L., 1990. Fundamentals of Metal Fatigue Analysis. Prentice Hall, New Jersey.

Bao, S., 2004. Two-parameter Characterization of Low Cycle, Hysteretic Fatigue Data. MS Thesis, Illinois Institute of Technology, Chicago, IL.

Bao, S., 2007. Fatigue, Mechanical and Magnetic Hysteresis. PhD Thesis, Illinois Institute of Technology, Chicago, IL.

Berktan, T., 1998. Piezomagnetism and Fatigue. MS Thesis, Illinois Institute of Technology, Chicago, IL.

Bily, M., 1993. Cyclic Deformation and Fatigue of Metals. Elsevier, Amsterdam, Germany.

Chrysochoos, A., Berthel, B., Latourte, F., Pagano, S., Wattrisse, B., Weber, B., 2008. Local energy approach to fatigue of steel. *Strain*, **44**(4):327-334. [doi:10.1111/j.1475-1305.2007.00381.x]

Desai, R.D., 1994. Origin and Inception of Fatigue Damage in Steel. MS Thesis, Illinois Institute of Technology, Chicago, IL.

Dieter, G.E., 1988. Mechanical Metallurgy. McGraw-Hill Book Company, New York, USA.

Erber, T., 2001. Hooke's law and fatigue limits in micromechanics. *European Journal of Physics*, **22**(5):491-499. [doi:10.1088/0143-0807/22/5/305]

Erber, T., Guralnick, S.A., Michels, S.C., 1993. Hysteresis and fatigue. *Annals of Physics*, **224**(2):157-192. [doi:10.1006/aphy.1993.1043]

Erber, T., Guralnick, S.A., Desai, R.D., Kwok, W., 1997. Piezomagnetism and fatigue. *Journal of Physics D: Applied Physics*, **30**(20):2818-2836.

Feltner, C., Morrow, J., 1961. Microplastic strain hysteresis energy as a criterion for fatigue fracture. *Journal of Basic Engineering, Transaction on ASME, Series D*, **83**:15-22.

Giancane, S., Chrysochoos, A., Dattoma, V., Wattrisse, B., 2009. Deformation and dissipated energies for high cycle fatigue of 2024-T3 aluminium alloy. *Theoretical and Applied Fracture Mechanics*, **52**(2):117-121. [doi:10.1016/j.tafmec.2009.08.004]

Giancane, S., Panella, F.W., Dattoma, V., 2010. Characterization of fatigue damage in long fiber epoxy composite laminates. *International Journal of Fatigue*, **32**(1):46-53. [doi:10.1016/j.ijfatigue.2009.02.024]

Guralnick, S.A., Bao, S., Erber, T., 2008. Piezomagnetism and fatigue: II. *Journal of Physics D: Applied Physics*, **41**(11):115006. [doi:10.1088/0022-3727/41/11/115006]

Halford, G.R., 1966. The energy required for fatigue. *Journal of Materials*, **1**(1):3-18.

Kachanov, L.M., 1986. Introduction to Continuum Damage Mechanics. Martinus Nijhoff, Dordrecht, the Netherlands.

Lemaitre, J., Chaboche, J.L., 1990. Mechanics of Solid Materials. Cambridge University Press, Cambridge, UK.

Martin, D., 1961. An energy criterion for low-cycle fatigue. *Journal of Basic Engineering, Transaction on ASME, Series D*, **83**:565-571.

Michels, S., 1991. Hysteresis and Fatigue. MS Thesis, Illinois Institute of Technology, Chicago, IL.

Miner, M.A., 1945. Cumulative Damage in Fatigue. *Journal of Applied Mechnics*, **12**:159-164.

Peyroux, R., Chrysochoos, A., Licht, C., Lobel, M., 1998. Thermomechanical coupling and pseudelasticity of shape memory alloys. *International Journal of Engineering Science*, **36**(4):489-509. [doi:10.1016/S0020-7225(97)00052-9]